

# Fractional reaction-subdiffusion equations: solution, stochastic paths, and applications

Sean D. Lawley\*

December 14, 2021

## Abstract

In contrast to normal diffusion, there is no canonical model for reactions between chemical species which move by anomalous subdiffusion. Indeed, the type of mesoscopic equation describing reaction-subdiffusion depends on subtle assumptions about the microscopic behavior of individual molecules. Furthermore, the correspondence between mesoscopic and microscopic models is not well understood. In this paper, we study the subdiffusion-limited model, which is defined by mesoscopic equations with fractional derivatives applied to both the movement and the reaction terms. Assuming that the reaction terms are affine functions, we show that the solution to the fractional system is the expectation of a random time change of the solution to the corresponding integer order system. This result yields a simple and explicit algebraic relationship between the fractional and integer order solutions in Laplace space. We then find the microscopic Langevin description of individual molecules that corresponds to such mesoscopic equations and give a computer simulation method to generate their stochastic trajectories. This analysis identifies some precise microscopic conditions that dictate when this type of mesoscopic model is or is not appropriate. We apply our results to several scenarios in cell biology which, despite the ubiquity of subdiffusion in cellular environments, have been modeled almost exclusively by normal diffusion. Specifically, we consider subdiffusive models of morphogen gradient formation, fluctuating mobility, and fluorescence recovery after photobleaching (FRAP) experiments. We also apply our results to fractional ordinary differential equations.

## 1 Introduction

Subdiffusion has been observed in very diverse systems [1, 2, 3, 4] and is especially prevalent in cell biology [5, 6]. Subdiffusion is defined by the following

---

\*Department of Mathematics, University of Utah, Salt Lake City, UT 84112 USA (lawley@math.utah.edu).

sublinear growth in the mean-squared displacement of a tracer particle,

$$\mathbb{E}[(Y(t) - Y(0))^2] \propto t^\alpha, \quad \alpha \in (0, 1), \quad (1)$$

where  $Y(t)$  is the one-dimensional position of the particle at time  $t \geq 0$  and  $\mathbb{E}$  denotes expectation.

A number of mathematical models yield the nonlinear phenomenon in (1), including continuous-time random walks, fractional Brownian motion, and random walks on fractal and disordered systems [5]. The continuous-time random walk model can be used to derive the following fractional diffusion equation [7],

$$\frac{\partial}{\partial t} c(x, t) = {}_0D_t^{1-\alpha} K \frac{\partial^2}{\partial x^2} c(x, t), \quad x \in \mathbb{R}, t > 0, \quad (2)$$

for the concentration  $c(x, t)$  of some chemical at position  $x$  at time  $t$ . In the mesoscopic description (2), the parameter  $K > 0$  is the generalized diffusivity (with dimensions  $(\text{length})^2(\text{time})^{-\alpha}$ ) and  ${}_0D_t^{1-\alpha}$  is the Riemann-Liouville fractional derivative [8],

$${}_0D_t^{1-\alpha} \phi(t) := \frac{d}{dt} \int_0^t \frac{1}{\Gamma(\alpha)(t-t')^{1-\alpha}} \phi(t') dt', \quad (3)$$

where  $\Gamma(\alpha)$  is the Gamma function.

An important and now longstanding question is how to model reaction kinetics for subdiffusive molecules (see the review [9] and [10, 11, 12, 13, 14, 15, 16, 17, 18, 19]). In contrast to normal diffusion, there is no canonical model for modeling reactions between subdiffusive molecules. Indeed, significantly different forms of reaction-subdiffusion equations have been proposed [9], and the structure of these mesoscopic equations depends on subtle assumptions about the microscopic behavior of individual molecules.

The following form of reaction-subdiffusion equations has been proposed for so-called subdiffusion-limited systems [20, 21, 9],

$$\frac{\partial}{\partial t} \mathbf{c} = {}_0D_t^{1-\alpha} \left( \text{diag}(K_1, \dots, K_n) \frac{\partial^2}{\partial x^2} \mathbf{c} + \mathbf{f}(\mathbf{c}) \right), \quad (4)$$

where  $\mathbf{c}$  is the vector of  $n$  chemical concentrations,

$$\mathbf{c}(x, t) = (c_i(x, t))_{i=1}^n \in \mathbb{R}^n,$$

with  $n$  generalized diffusivities,  $K_1, \dots, K_n$ , and

$$\mathbf{f} : \mathbb{R}^n \mapsto \mathbb{R}^n$$

describes reactions between the  $n$  species. Importantly, the fractional operator  ${}_0D_t^{1-\alpha}$  is applied to both the movement and the reaction terms in the righthand side of (4). Models of the form (4) have been derived from continuous-time random walks [20], particularly those with instantaneous creation and annihilation [22]. Such models have also been proposed to describe the numerical simulations

of [21]. Similar models have been used to study subdiffusive bimolecular reactions [21, 23, 24, 14], subdiffusive pattern formation [25], and traveling waves in subdiffusive media [26, 27]. We note that (4) is sometimes written with  $\frac{\partial}{\partial t}$  replaced by the Caputo derivative and  ${}_0D_t^{1-\alpha}$  replaced by the identity [9].

Many fundamental questions regarding (4) remain unanswered. What is the solution to (4)? How can we investigate stability? What does (4) imply about the stochastic movement and reactions of single molecules? How can one simulate the stochastic trajectories of individual molecules described by (4)? What are some biophysical implications for a system following (4)?

In this paper, we answer these questions for a more general version of the equations in (4) in the case that  $\mathbf{f}$  is an affine function of  $\mathbf{c}$ . In particular, we consider fractional equations of the general form

$$\frac{\partial}{\partial t}\mathbf{c} = \mathcal{D}(\mathcal{A}\mathbf{c} + \mathbf{r}), \quad x \in V \subseteq \mathbb{R}^d, t > 0. \quad (5)$$

In (5),  $V \subseteq \mathbb{R}^d$  is a  $d$ -dimensional spatial domain (if  $V$  has a boundary, then we also impose boundary conditions) and  $\mathcal{D}$  is the following integro-differential operator,

$$\mathcal{D}\phi(t) = \frac{d}{dt} \int_0^t M(t-t')\phi(t') dt', \quad (6)$$

where  $M(t)$  is some given memory kernel (notice that (6) reduces to (3) if  $M(t) = \frac{1}{\Gamma(\alpha)t^{1-\alpha}}$ ). Further,

$$\mathbf{r} = \mathbf{r}(x) \in \mathbb{R}^n$$

is a space-dependent, time-independent vector, and  $\mathcal{A}$  is a linear, spatial operator.

The main example that we have in mind is where  $\mathbf{r} \equiv 0$  and  $\mathcal{A}$  is the diffusion-advection-reaction operator,

$$\mathcal{A}\mathbf{c} = (\text{diag}(\mathbb{L}_1, \dots, \mathbb{L}_n) + R(x))\mathbf{c} = \begin{pmatrix} \mathbb{L}_1 c_1 \\ \vdots \\ \mathbb{L}_n c_n \end{pmatrix} + R(x)\mathbf{c}, \quad (7)$$

where

$$R(x) : \bar{V} \mapsto \mathbb{R}^{n \times n} \quad (8)$$

is a space-dependent matrix and  $\mathbb{L}_1, \dots, \mathbb{L}_n$  are  $n$  forward Fokker-Planck operators, each of the form

$$\mathbb{L}_i f(x) := - \sum_{j=1}^d \frac{\partial}{\partial x_j} [\mu_j(x, i) f(x)] + \frac{1}{2} \sum_{j=1}^d \sum_{k=1}^d \frac{\partial^2}{\partial x_j \partial x_k} [(\sigma(x, i) \sigma(x, i)^\top)_{j,k} f(x)], \quad (9)$$

where  $\mu(x, i) \in \mathbb{R}^d$  is the external force (drift) vector and  $\sigma(x, i) \in \mathbb{R}^{d \times m}$  describes the space-dependence and anisotropy in the diffusivity for each chemical species  $i \in \{1, \dots, n\}$ . In this case,  $R(x)$  describes the reactions between the  $n$  chemical species and  $\mathbb{L}_i$  describes the movement of the  $i$ th species. In the absence of reactions, such equations as (5)-(9) are called fractional Fokker-Planck equations [28]. Notice that (5)-(9) becomes (4) if  $d = 1$ ,  $V = \mathbb{R}$ ,  $\mu(x, i) = 0$ ,  $\sigma(x, i) = \sqrt{2K_i}$ , and  $\mathbf{f}(\mathbf{c}) = R(x)\mathbf{c}$ .

The rest of the paper is organized as follows. In section 2, we show that the solution to (5) is

$$\mathbf{c}(x, t) = \mathbb{E}[\mathbf{u}(x, S(t))], \quad (10)$$

where  $\mathbf{u}(x, s)$  satisfies the corresponding integer order equation (namely (5) with  $\mathcal{D}$  replaced by the identity) and  $S(t)$  is the inverse of a Lévy subordinator with Laplace exponent  $\Psi(\lambda)$  given by the reciprocal of the Laplace transform of the memory kernel in the integro-differential operator  $\mathcal{D}$  in (6),

$$\Psi(\lambda) = \frac{1}{\widehat{M}(\lambda)},$$

where the Laplace transform in time is denoted by

$$\widehat{\phi}(\lambda) := \int_0^\infty e^{-\lambda t} \phi(t) dt.$$

We obtain (10) by proving the following algebraic relationship between  $\mathbf{c}$  and  $\mathbf{u}$  in Laplace space,

$$\widehat{\mathbf{c}}(x, \lambda) = \frac{\Psi(\lambda)}{\lambda} \widehat{\mathbf{u}}(x, \Psi(\lambda)). \quad (11)$$

We also show how (10) yields a sufficient condition for stability when the reactions in (5) are nonlinear. In section 3, we give the stochastic Langevin representation of individual molecules described by (5) with  $\mathcal{A}$  in (7)-(9). Specifically, we construct a stochastic process whose probability density satisfies (5)-(9) when  $R(x)$  has a certain probabilistic structure. In this section, we also give a stochastic simulation algorithm to generate realizations of the stochastic process underlying (5). In section 4, we apply our results to some examples of biophysical interest. In particular, we analyze subdiffusive models of protein gradient formation, stochastically switching mobility, and fluorescence recovery after photobleaching (FRAP) experiments. In section 5, we apply our results to fractional ordinary differential equations (ODEs). We conclude by discussing related work and future directions.

## 2 Exact solution

In this section, we show that (10) satisfies the fractional equations in (5) if  $\mathbf{u}(x, s)$  satisfies the corresponding integer order equations. The main rigorous result is

Theorem 1 in section 2.1, which makes no reference to (5). Instead, Theorem 1 is a general result about the Laplace transform of any function subordinated by a continuous, inverse Lévy subordinator (as in (10)), assuming the function satisfies a mild integrability assumption (see (15)). In section 2.2, we then show formally how Theorem 1 implies that (10) satisfies (5). In sections 2.3-2.4, we work out some implications of this result.

## 2.1 Main theorem

Let the following stochastic process

$$T = \{T(s)\}_{s \geq 0}$$

be a Lévy subordinator. That is,  $T$  is a one-dimensional, nondecreasing Lévy process with  $T(0) = 0$  [29, 30]. For each fixed  $s > 0$ , assume that  $T(s)$  is a continuous random variable, which means

$$\mathbb{P}(T(s) = t) = 0, \quad \text{for all } s > 0 \text{ and } t \geq 0. \quad (12)$$

Let  $\Psi(\lambda)$  denote the Laplace exponent of  $T$ , which means that for all  $s \geq 0$  and  $\lambda \geq 0$ ,

$$\begin{aligned} \mathbb{E}[e^{-\lambda T(s)}] &= e^{-s\Psi(\lambda)}, \\ \Psi(\lambda) &= b\lambda + \int_0^\infty (1 - e^{-\lambda z}) \nu(dz), \end{aligned} \quad (13)$$

where  $b \geq 0$  is the drift of  $T$  and  $\nu$  is the Lévy measure of  $T$ . In particular,  $\nu$  satisfies  $\nu((-\infty, 0)) = 0$  and

$$\int_0^\infty \min\{1, z\} \nu(dz) < \infty.$$

Let  $S = \{S(t)\}_{t \geq 0}$  be the inverse subordinator of  $T$ ,

$$S(t) := \inf\{s > 0 : T(s) > t\}. \quad (14)$$

Notice that  $S(0) = T(0) = 0$  almost surely. Notice also that paths of  $S$  are almost surely continuous functions of  $t$ , since (12) implies that paths of  $T$  are almost surely strictly increasing functions of  $s$ .

**Theorem 1.** *Let*

$$\mathbf{u}(s) = (u_i(s))_{i=1}^n : [0, \infty) \mapsto \mathbb{R}^n,$$

*be a given function of time. Fix  $\lambda > 0$  and assume that for each component  $i \in \{1, \dots, n\}$ ,*

$$\int_0^\infty e^{-\lambda t} \mathbb{E}|u_i(S(t))| dt < \infty. \quad (15)$$

If we define

$$\mathbf{c}(t) := \mathbb{E}[\mathbf{u}(S(t))], \quad \text{for } t \geq 0,$$

then

$$\lambda \widehat{\mathbf{c}}(\lambda) = \Psi(\lambda) \widehat{\mathbf{u}}(\Psi(\lambda)).$$

The proof of Theorem 1 relies on the following lemma. We write

$$\tau =_{\text{d}} \exp(\lambda)$$

to denote that  $\tau$  is exponentially distributed with rate  $\lambda > 0$ , which means  $\mathbb{P}(\tau > t) = e^{-\lambda t}$  for each  $t > 0$ .

**Lemma 2.** *If  $\tau =_{\text{d}} \exp(\lambda)$  and is independent of  $T$ , then*

$$S(\tau) =_{\text{d}} \exp(\Psi(\lambda)).$$

*Proof of Lemma 2.* Fix  $s > 0$ . Using the definition of  $S(t)$  in (14) and the independence of  $T$  and  $\tau$ , conditioning on the value of  $\tau$  gives

$$\mathbb{P}(S(\tau) > s) = \int_0^\infty F(t) \lambda e^{-\lambda t} dt, \quad (16)$$

where  $F(t) := \mathbb{P}(T(s) \leq t)$  and we have used (12). Integrating by parts in (16) yields

$$\int_0^\infty F(t) \lambda e^{-\lambda t} dt = \int_0^\infty e^{-\lambda t} dF(t), \quad (17)$$

since  $\lim_{t \rightarrow \infty} e^{-\lambda t} F(t) = 0$  and  $F(0) = \mathbb{P}(T(s) \leq 0) = 0$  by (12) since  $s > 0$ . Now, (13) implies that the Riemann-Stieltjes integral in the righthand side of (17) is

$$\int_0^\infty e^{-\lambda t} dF(t) = \mathbb{E}[e^{-\lambda T(s)}] = e^{-s\Psi(\lambda)}. \quad (18)$$

Combining (16)-(18) completes the proof.  $\square$

The proof of Theorem 1 follows quickly from Lemma 2.

*Proof of Theorem 1.* The Laplace transform of  $\mathbf{c}(t)$  is

$$\begin{aligned} \widehat{\mathbf{c}}(\lambda) &= \int_0^\infty e^{-\lambda t} \mathbf{c}(t) dt = \int_0^\infty e^{-\lambda t} \mathbb{E}[\mathbf{u}(S(t))] dt \\ &= \mathbb{E} \int_0^\infty e^{-\lambda t} \mathbf{u}(S(t)) dt = \frac{1}{\lambda} \mathbb{E}[\mathbf{u}(S(\tau))], \end{aligned}$$

where  $\tau =_{\text{d}} \exp(\lambda)$  is independent of  $S$  (the assumption (15) and the theorems of Tonelli and Fubini ensure the validity of exchanging  $\mathbb{E}$  with the integral). Therefore, if  $\sigma =_{\text{d}} \exp(\Psi(\lambda))$ , then Lemma 2 implies that

$$\widehat{\mathbf{c}}(\lambda) = \frac{1}{\lambda} \mathbb{E}[\mathbf{u}(\sigma)] = \frac{1}{\lambda} \int_0^\infty \Psi(\lambda) e^{-\Psi(\lambda)t} \mathbf{u}(t) dt = \frac{\Psi(\lambda)}{\lambda} \widehat{\mathbf{u}}(\Psi(\lambda)), \quad (19)$$

which completes the proof.  $\square$

## 2.2 Fractional equations

We now use Theorem 1 to solve fractional equations. Consider the fractional system,

$$\begin{aligned} \frac{\partial}{\partial t} \mathbf{c} &= \mathcal{D}(\mathcal{A}\mathbf{c} + \mathbf{r}), \quad x \in V \subseteq \mathbb{R}^d, t > 0, \\ \mathbf{c}(x, 0) &= \mathbf{c}_{\text{init}}(x), \end{aligned} \quad (20)$$

where  $V \subseteq \mathbb{R}^d$  is some  $d$ -dimensional spatial domain and the initial condition  $\mathbf{c}_{\text{init}}$  is a given bounded function of space. Assume  $\mathcal{D}$  is the integro-differential operator in (6) with memory kernel  $M(t)$  defined by its Laplace transform,

$$\widehat{M}(\lambda) = \frac{1}{\Psi(\lambda)}, \quad (21)$$

and assume  $M$  is sufficiently regular so that

$$\lim_{t \rightarrow 0^+} \int_0^t M(t') dt' = 0. \quad (22)$$

Assume the operator  $\mathcal{A}$  commutes with scalar multiplication, Laplace transforms in time, and the fractional temporal operator  $\mathcal{D}$ . That is, assume

$$\mathcal{A}\beta\mathbf{w}(x, t) = \beta\mathcal{A}\mathbf{w}(x, t), \quad (23)$$

$$\widehat{(\mathcal{A}\mathbf{w})}(x, \lambda) = \mathcal{A}\widehat{\mathbf{w}}(x, \lambda), \quad (24)$$

$$\mathcal{D}\mathcal{A}\mathbf{w}(x, t) = \mathcal{A}\mathcal{D}\mathbf{w}(x, t), \quad (25)$$

for scalar constants  $\beta > 0$  and functions

$$\mathbf{w} : \overline{V} \times [0, \infty) \mapsto \mathbb{R}^n$$

in the domain of  $\mathcal{A}$ . For example, if  $\mathcal{A}$  is a sufficiently regular linear differential operator acting on the spatial variable  $x$  (as in (7)), then (23)-(25) hold. More generally,  $\mathcal{A}$  could be a linear integro-differential operator acting on  $x$ . In addition,  $\mathcal{A}$  need not even act on  $x$ , but could instead simply be a matrix  $\mathcal{A} = R \in \mathbb{R}^{n \times n}$ , in which case (20) becomes a system of fractional ODEs (see section 5).

Suppose  $\mathbf{u}(x, s) = (u_i(x, s))_{i=1}^n$  satisfies the system of integer order equations corresponding to (20) with the same initial condition,

$$\begin{aligned} \frac{\partial}{\partial s} \mathbf{u} &= \mathcal{A}\mathbf{u} + \mathbf{r}, \quad x \in V \subseteq \mathbb{R}^d, s > 0, \\ \mathbf{u}(x, 0) &= \mathbf{c}_{\text{init}}(x). \end{aligned} \quad (26)$$

Assuming that (20) and (26) are sufficiently regular to admit Laplace transformation, we claim that the following definition of  $\mathbf{c}(x, t)$  satisfies (20),

$$\mathbf{c}(x, t) := \mathbb{E}[\mathbf{u}(x, S(t))]. \quad (27)$$

To see this, we work with the Laplace transforms of (20) and (26), which are

$$\lambda \widehat{\mathbf{c}}(x, \lambda) - \mathbf{c}_{\text{init}}(x) = \frac{\lambda}{\Psi(\lambda)} \left[ \mathcal{A} \widehat{\mathbf{c}}(x, \lambda) + \frac{\mathbf{r}(x)}{\lambda} \right], \quad (28)$$

$$\lambda \widehat{\mathbf{u}}(x, \lambda) - \mathbf{c}_{\text{init}}(x) = \mathcal{A} \widehat{\mathbf{u}}(x, \lambda) + \frac{\mathbf{r}(x)}{\lambda}. \quad (29)$$

In obtaining (28)-(29), we used (23)-(25) and that

$$\widehat{\mathcal{D}}\mathbf{c} = \frac{\lambda}{\Psi(\lambda)} \widehat{\mathbf{c}}, \quad \widehat{\mathcal{D}}\mathbf{r} = \frac{\lambda}{\Psi(\lambda)} \widehat{\mathbf{r}} = \frac{\mathbf{r}}{\Psi(\lambda)},$$

which follows from the convolution form of  $\mathcal{D}$  in (6), the relation in (21), and (22). Now, it is a straightforward algebra exercise to use (23)-(25) to show that if  $\widehat{\mathbf{u}}$  satisfies (29) and  $\widehat{\mathbf{c}}$  and  $\widehat{\mathbf{u}}$  satisfy the following relation,

$$\lambda \widehat{\mathbf{c}}(x, \lambda) = \Psi(\lambda) \widehat{\mathbf{u}}(x, \Psi(\lambda)), \quad (30)$$

then  $\widehat{\mathbf{c}}$  satisfies (28). Of course, (30) is precisely the relation found in Theorem 1 for each fixed  $x \in \bar{V}$ .

Summarizing, if we define  $\mathbf{c}$  by (27), then Theorem 1 implies that  $\mathbf{c}$  and  $\mathbf{u}$  satisfy (30). Therefore, if  $\mathbf{u}$  satisfies the Laplace space equation in (29) (which is equivalent to (26)), then  $\mathbf{c}$  satisfies the Laplace space equation in (28). But, the Laplace space equation (28) is equivalent to (20). Hence,  $\mathbf{c}$  satisfies (20) as desired.

### 2.3 Boundary conditions

In the case that the spatial domain  $V \subseteq \mathbb{R}^d$  is bounded, we impose boundary conditions. Suppose the solution  $\mathbf{u}(x, s)$  to (26) satisfies boundary conditions of the form,

$$A(x) \frac{\partial}{\partial \mathbf{n}} \mathbf{u}(x, s) + B(x) \mathbf{u}(x, s) = \mathbf{v}(x), \quad x \in \partial V, \quad (31)$$

where  $\frac{\partial}{\partial \mathbf{n}}$  denotes differentiation with respect to the normal derivative,  $A(x), B(x) \in \mathbb{R}^{n \times n}$  are given space-dependent matrices, and  $\mathbf{v}(x) \in \mathbb{R}^n$  is a given space-dependent vector. Then, it is immediate that  $\mathbf{c}(x, t) := \mathbb{E}[\mathbf{u}(x, S(t))]$  satisfies the boundary conditions in (31) assuming sufficient regularity to interchange  $\frac{\partial}{\partial \mathbf{n}}$  with  $\mathbb{E}$ . Similarly, if  $V \subseteq \mathbb{R}^d$  is unbounded, then appropriate growth conditions on  $\mathbf{u}$  also apply to  $\mathbf{c}$ .

### 2.4 Stability for nonlinear reactions

The formula (27) relates the fractional order solution  $\mathbf{c}$  to the integer order solution  $\mathbf{u}$ . It follows from (27) that if  $\mathbf{u}$  approaches a finite steady-state,

$$\mathbf{u}_{\text{ss}}(x) := \lim_{s \rightarrow \infty} \mathbf{u}(x, s) \in \mathbb{R}^n, \quad (32)$$

then  $\mathbf{c}$  inherits this same finite steady-state,

$$\lim_{t \rightarrow \infty} \mathbf{c}(x, t) = \mathbf{u}_{\text{ss}}(x). \quad (33)$$

To see this, fix  $x \in \bar{V}$  and let  $\mathbf{u}(x, s)$  be any bounded function of time  $s \in [0, \infty)$  satisfying (32). Since  $S(t) \rightarrow \infty$  as  $t \rightarrow \infty$  with probability one, the Lebesgue dominated convergence theorem yields (33). We emphasize that the limit in (32) is assumed to be finite, since it is possible for  $\mathbf{u}$  to diverge and  $\mathbf{c}$  to approach a finite limit (see section 5 below).

An important consequence of the simple observation in (33) is that stability of equilibria for fractional equations with *nonlinear* reactions can be deduced from stability of the corresponding integer order equations. To see this, consider the system of fractional equations,

$$\frac{\partial}{\partial t} \mathbf{c} = \mathcal{D}(\mathcal{A}\mathbf{c} + \mathbf{f}(\mathbf{c})), \quad (34)$$

where  $\mathbf{f} : \mathbb{R}^n \mapsto \mathbb{R}^n$  is some nonlinear function of  $\mathbf{c}$ . Suppose that this system has a steady-state,  $\mathbf{c}_{\text{ss}} \in \mathbb{R}^n$ , with  $\mathbf{f}(\mathbf{c}_{\text{ss}}) = \mathcal{A}\mathbf{c}_{\text{ss}} = 0$ . Considering a small perturbation,  $\mathbf{c}(x, t) = \mathbf{c}_{\text{ss}} + \varepsilon \mathbf{b}(x, t)$ , with  $\varepsilon \ll 1$  yields the following leading order equation for  $\mathbf{b}$ ,

$$\frac{\partial}{\partial t} \mathbf{b} = \mathcal{D}(\mathcal{A}\mathbf{b} + R_{\mathbf{f}}\mathbf{b}), \quad (35)$$

where  $R_{\mathbf{f}} \in \mathbb{R}^{n \times n}$  is the Jacobian of  $\mathbf{f}$  evaluated at  $\mathbf{c}_{\text{ss}}$ . Since (35) is linear, the solution is  $\mathbf{b}(x, t) = \mathbb{E}[\mathbf{u}(x, S(t))]$  where  $\mathbf{u}(x, s)$  satisfies (35) with  $\mathcal{D}$  replaced by the identity. Hence, if  $\lim_{s \rightarrow \infty} \mathbf{u}(x, s) = 0$ , then we conclude that  $\lim_{t \rightarrow \infty} \mathbf{b}(x, t) = 0$ , and thus the steady-state,  $\mathbf{c}_{\text{ss}}$ , for the fractional nonlinear equation is stable. Now, the equation for  $\mathbf{u}$  is the linearization of (34) with  $\mathcal{D}$  replaced by the identity. Therefore, we conclude that the linear stability of a nonlinear, integer order equation implies the linear stability of the corresponding nonlinear, fractional order equation. However, we caution that stability of a fractional equation does not imply stability of the corresponding integer order equation (see section 5 below). Summarizing, stability of an integer order equation is a sufficient (but not necessary) condition for stability of the corresponding fractional equation.

### 3 Stochastic representation

In this section, we construct a stochastic process whose probability density satisfies (5) in the case that  $\mathbf{r} \equiv 0$  and the operator  $\mathcal{A}$  is given by (7) and the reaction matrix  $R(x)$  has a certain probabilistic structure. In particular, we assume that for each  $x \in \bar{V} \subseteq \mathbb{R}^d$ , the matrix  $R(x)$  has nonnegative off-diagonal entries (meaning  $R(x)$  is a so-called Metzler matrix [31]) and the diagonal entries are such that each column of  $R(x)$  sums to zero.

### 3.1 Internal Markov process

Let  $\{(X(s), I(s))\}_{s \geq 0}$  be a Markov process on the state space  $\bar{V} \times \{1, \dots, n\}$  with infinitesimal generator  $\mathcal{G}$  defined by

$$\mathcal{G}f(x, i) = \mathbb{L}_i^* f(x, i) + \sum_{j=1}^n (R^\top(x))_{i,j} f(x, j),$$

where  $\mathbb{L}_i^*$  is the formal adjoint of  $\mathbb{L}_i$  in (9) and  $R^\top$  is the transpose of  $R$ , meaning  $(R^\top(x))_{i,j} = (R(x))_{j,i}$ . The generator  $\mathcal{G}$  acts on functions  $f(x, i) : \bar{V} \times \{1, \dots, n\} \mapsto \mathbb{R}$  which are twice-continuously differentiable in  $x$ . In the language of Markov processes,  $\mathcal{G}$  is the backward operator corresponding to the forward operator  $\mathcal{A}$ .

Under these assumptions,  $\{I(s)\}_{s \geq 0}$  is a continuous-time jump process on  $\{1, \dots, n\}$  that jumps from state  $I(s) = i$  to state  $j \neq i$  at rate  $(R(X(s)))_{j,i} \geq 0$  at time  $s \geq 0$ . Furthermore,  $\{X(s)\}_{s \geq 0}$  satisfies the stochastic differential equation (SDE),

$$dX(s) = \mu(X(s), I(s)) ds + \sigma(X(s), I(s)) dW(s), \quad (36)$$

where  $\{W(s)\}_{s \geq 0}$  is a standard  $m$ -dimensional Brownian motion.

In words,  $X(s)$  satisfies an SDE whose righthand side switches according to the jump process  $I(s)$ , and the jump rates of  $I(s)$  may depend on the position  $X(s)$ . The process  $(X(s), I(s))$  is sometimes called a hybrid switching diffusion [32]. The word “hybrid” is used because the process combines the continuous dynamics of  $X(s)$  with the discrete dynamics of  $I(s)$ .

Let  $\mathbf{q}_i(x, s)$  be the probability density that  $X(s) = x$  and  $I(s) = i$ . If we define the vector  $\mathbf{q}(x, s) = (\mathbf{q}_i(x, s))_{i=1}^n \in \mathbb{R}^n$ , then the forward Fokker-Planck equation for  $\mathbf{q}$  is

$$\frac{\partial}{\partial s} \mathbf{q} = \mathcal{A} \mathbf{q}, \quad x \in V \subseteq \mathbb{R}^d, \quad s > 0. \quad (37)$$

In the case that  $V$  has a boundary, boundary conditions are imposed on  $\mathbf{q}$  corresponding to the assumed behavior of  $X(s)$  on the boundary. For example, if  $X(s)$  reflects from some portion of the boundary  $\partial V_0 \subseteq \partial V$  when  $I(s) = i$ , then

$$\frac{\partial}{\partial \mathbf{n}} \mathbf{q}_i(x, s) = 0, \quad x \in \partial V_0.$$

Alternatively, if  $X(s)$  is absorbed at  $\partial V_0$  when  $I(s) = i$ , then

$$\mathbf{q}_i(x, s) = 0, \quad x \in \partial V_0.$$

### 3.2 Random time changed process

Let  $\{S(t)\}_{t \geq 0}$  be the inverse subordinator in (14) that is taken to be independent of  $\{(X(s), I(s))\}_{s \geq 0}$ . Define the stochastic process

$$(Y(t), J(t)) := (X(S(t)), I(S(t))), \quad t \geq 0. \quad (38)$$

Let  $\mathbf{p}_i(x, t)$  be the probability density that  $Y(t) = x$  and  $J(t) = i$  and define the vector  $\mathbf{p}(x, s) = (\mathbf{p}_i(x, s))_{i=1}^n$ . By conditioning on the value of  $S(t)$  and using independence, it follows that

$$\mathbf{p}(x, t) = \mathbb{E}[\mathbf{q}(x, S(t))].$$

Therefore, our analysis in section 2 yields

$$\frac{\partial}{\partial t} \mathbf{p} = \mathcal{D} \mathbf{A} \mathbf{p}, \quad x \in V \subseteq \mathbb{R}^d, t > 0, \quad (39)$$

and  $\mathbf{p}$  satisfies the same boundary conditions as  $\mathbf{q}$ .

Summarizing, the (mesoscopic) fractional reaction-subdiffusion equations in (39) describe (microscopic) individual stochastic molecules which evolve according to (38). In particular,  $Y(t)$  denotes the spatial position of a particle and  $J(t)$  denotes its discrete state. We now investigate the dynamics of  $(Y(t), J(t))$  to understand what fractional reaction-diffusion equations of the form (39) imply about the dynamics of individual molecules.

We see from (38) and (36) that the particle subdiffuses with dynamics that switch according to its discrete state. In particular, the path of  $Y(t)$  follows the path of  $X(s)$ , but the motion of  $Y(t)$  is punctuated by “pauses” of the inverse subordinator  $S(t)$  (which correspond to jumps of the subordinator  $T(s)$ , see section 4.2). Analogously,  $J(t)$  follows the path of  $I(s)$ , but  $J(t)$  pauses when  $S(t)$  pauses. Importantly, notice that  $J(t)$  pauses exactly when  $Y(t)$  pauses, and therefore  $J(t)$  cannot jump when  $Y(t)$  is paused. Hence, we obtain one simple microscopic property implied by the mesoscopic equations in (39).

Next, we investigate the time between jumps of  $J(t)$ . In the case that  $R(x)$  is constant in space, the jump times of  $I(s)$  are exactly exponentially distributed. In particular, the time that  $I(s)$  spends in state  $i$  is an exponential random variable with rate  $\lambda_i := \sum_{j \neq i} R_{j,i}$ . Letting  $\sigma$  denote this exponential time, it follows that  $J(t)$  spends time  $T(\sigma)$  in state  $i$ . We thus obtain an additional microscopic property implied by the mesoscopic equations in (39).

Moreover, we can compute the probability distribution for the sojourn time  $T(\sigma)$  in the typical case that the fractional operator is the Riemann-Liouville derivative,  $\mathcal{D} = {}_0D_t^{1-\alpha}$  in (3) with  $\alpha \in (0, 1)$ . In this case, the subordinator  $T$  is an  $\alpha$ -stable subordinator. A direct calculation shows that this random time has the following distribution [33, 34],

$$\mathbb{P}(T(\sigma) > t) = E_\alpha(-\lambda_i t^\alpha), \quad t > 0, \quad (40)$$

where  $E_\alpha$  is the Mittag-Leffler function,

$$E_\alpha(z) := \sum_{k=0}^{\infty} \frac{z^k}{\Gamma(1 + \alpha k)}.$$

Hence, a microscopic condition implied by the mesoscopic equations in (39) in this case is that the particle switches states at Mittag-Leffler distributed times described by (40).

### 3.3 Stochastic simulation

Having constructed the stochastic process  $(Y(t), J(t))$  in (38) that corresponds to the fractional equations (39), we can simulate stochastic paths of this process. This simulation involves two main steps: (i) approximating the path of the internal Markov process  $\{(X(s_k), I(s_k))\}_k$  on some internal time mesh  $\{s_k\}_k$ , and (ii) approximating the path of the inverse subordinator  $\{S(t_k)\}_k$  on some time mesh  $\{t_k\}_k$ .

Step (i) is well-studied. For example, see Chapter 5 in [32]. Furthermore, if the transition rate matrix is constant ( $R(x) \equiv R$ ), then step (i) entails merely simulating paths of  $I(s)$  (which can be done exactly and efficiently with the Gillespie algorithm [35]) and simulating paths of  $X(s)$  between jumps of  $I(s)$ , which can be done with any simulation method for SDEs (see [36]).

Step (ii) depends on the particular subordinator  $T(s)$  under consideration. In the case that  $T(s)$  is an  $\alpha$ -stable subordinator, Magdziarz et al. [37] developed an efficient algorithm for simulating paths of  $T(s)$  and  $S(t)$ . Carnaffan and Kawai [38] developed methods for simulating paths of  $T(s)$  and  $S(t)$  for the cases that  $T(s)$  is a tempered stable subordinator or a gamma subordinator.

Having obtained the simulated values  $\{(X(s_k), I(s_k))\}_k$  and  $\{S(t_k)\}_k$  by the methods just referenced, one can obtain  $X(S(t_k))$  from a simple linear interpolation between  $X(s_{\bar{k}})$  and  $X(s_{\bar{k}+1})$ , where the index  $\bar{k}$  is chosen so that  $s_{\bar{k}} \leq S(t_k) \leq s_{\bar{k}+1}$ . Similarly, one can set  $J(S(t_k)) = I(s_{\tilde{k}})$  where  $\tilde{k}$  is the largest index such that  $s_{\tilde{k}} \leq S(t_k)$ . We illustrate this method in section 4.2 below.

## 4 Biophysical applications

We now apply our results to some biophysical systems which have typically been modeled by normal diffusion.

### 4.1 Subdiffusive morphogen gradient formation

The formation of morphogen gradients, such as the bicoid gradient of *Drosophila*, is often modeled by diffusion away from a localized source and subsequent degradation. The degradation often results from binding to receptors in the cell membrane [39]. The basic theory can be illustrated with a reaction-diffusion equation [40],

$$\frac{\partial}{\partial s} u = D \frac{\partial^2}{\partial x^2} u - ku, \quad x > 0, s > 0, \quad (41)$$

modeling the protein (morphogen) concentration  $u(x, s)$  at position  $x$  at time  $s$ , which diffuses with diffusivity  $D > 0$  and degrades at rate  $k > 0$ . The protein source can be modeled by specifying a constant flux  $\varphi > 0$  boundary condition

at  $x = 0$ ,

$$-D \frac{\partial}{\partial x} u = \varphi > 0, \quad x = 0, \quad (42)$$

and it is assumed that there is no protein initially,

$$u = 0, \quad s = 0. \quad (43)$$

The solution to (41)-(43) is [41]

$$u(x, s) = u_{\text{ss}}(x) \left[ 1 - \frac{1}{2} \operatorname{erfc} \left( \sqrt{\bar{s}} - \frac{\bar{x}}{\sqrt{4\bar{s}}} \right) - \frac{e^{2\bar{x}}}{2} \operatorname{erfc} \left( \sqrt{\bar{s}} + \frac{\bar{x}}{\sqrt{4\bar{s}}} \right) \right], \quad (44)$$

where  $\bar{x} = (\sqrt{k/D})x$  and  $\bar{s} = ks$  are dimensionless space and time variables and the steady-state solution is the decaying exponential,

$$u_{\text{ss}}(x) = \frac{\varphi}{\sqrt{Dk}} e^{-\bar{x}}. \quad (45)$$

A common tool to characterize the time it takes the time-dependent gradient (44) to approach the steady-state gradient (45) is the *accumulation time* [40, 42]. The accumulation time  $\tau(x)$  is defined by

$$\tau(x) := \int_0^\infty -s \frac{\partial R}{\partial s}(x, s) ds = \int_0^\infty R(x, s) ds, \quad (46)$$

where  $R(x, s)$  is the local relaxation function which measures the approach of  $u(x, s)$  to  $u_{\text{ss}}(x)$ ,

$$R(x, s) = \frac{u(x, s) - u_{\text{ss}}(x)}{u(x, 0) - u_{\text{ss}}(x)} = 1 - \frac{u(x, s)}{u_{\text{ss}}(x)}. \quad (47)$$

The relaxation function  $R(x, s)$  is similar to a survival probability, and thus the accumulation time  $\tau(x)$  is analogous to a mean first passage time [40, 42]. Using (44), it is straightforward to calculate that (46) is

$$\tau(x) = \frac{1}{2k} (1 + (\sqrt{k/D})x).$$

We can now use the analysis in sections 2-3 above to investigate how this standard theory is modified if the proteins move subdiffusively and the degradation is subdiffusion-limited. Indeed, since degradation requires that a protein reaches a receptor, it is quite plausible that the degradation could be limited by the subdiffusive proteins. Analogous to (41)-(42), the subdiffusive protein concentration  $c(x, t)$  now satisfies

$$\begin{aligned} \frac{\partial}{\partial t} c &= \mathcal{D} \left( D \frac{\partial^2}{\partial x^2} c - kc \right), \quad x > 0, t > 0, \\ -D \frac{\partial}{\partial x} c &= \varphi_0 > 0, \quad x = 0, \\ c &= 0, \quad t = 0, \end{aligned} \quad (48)$$

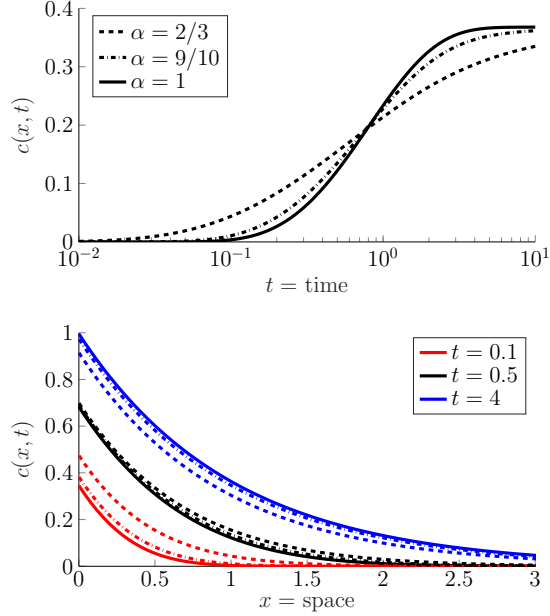


Figure 1: Diffusive and subdiffusive gradient formation. The top panel plots the solution  $c(x, t)$  to (48) as a function of time at  $x = 1$ . The dashed curve is for  $\alpha = 2/3$ , the dot-dashed curve is for  $\alpha = 9/10$ , and the solid curve is normal diffusion ( $\alpha = 1$ ). The bottom panel plots  $c(x, t)$  as a function of  $x$  for  $t = 0.1, 0.5, 4$ . The dashed, dot-dashed, and solid curves in the bottom panel correspond respectively to  $\alpha = 2/3$ ,  $\alpha = 9/10$ , and  $\alpha = 1$ , as in the top panel. See the text for more details.

for some integro-differential operator  $\mathcal{D}$  as in (6). Note that the parameters  $D$  and  $k$  in (41)-(42) necessarily differ from the  $D$  and  $k$  in (48) (they have different units), but we keep the same notation for simplicity. To solve (48), we take the Laplace transform of the time-dependent diffusive solution in (44) and use the relation (30) of section 2 above to obtain the Laplace transform of the solution to (48),

$$\hat{c}(x, \lambda) = \frac{\Psi(\lambda)}{\lambda} \hat{u}(x, \Psi(\lambda)) = u_{\text{ss}}(x) \frac{\exp(\bar{x}(1 - \sqrt{1 + \Psi(\lambda)/k}))}{\lambda \sqrt{1 + \Psi(\lambda)/k}}, \quad (49)$$

where  $\Psi(\lambda)$  is the Laplace exponent corresponding to  $\mathcal{D}$  (see section 2.1). Multiplying (49) by  $\lambda$  and using that  $\Psi(\lambda) \rightarrow 0$  as  $\lambda \rightarrow 0$  and the final value theorem of Laplace transforms confirms the desired result that  $c(x, t) \rightarrow u_{\text{ss}}(x)$  as  $t \rightarrow \infty$ . That is, the steady-state behavior of the subdiffusive solution is identical to the steady-state behavior of the diffusive solution. This result can also be seen from (32)-(33) in section 2.4 above.

We are not able to analytically invert the Laplace transform in (49). Nevertheless, for a particular choice of  $\Psi(\lambda)$ , it is straightforward to numerically invert

(49) to obtain  $c(x, t)$ . In Figure 1, we plot the protein concentration for the Laplace exponent,

$$\Psi(\lambda) = \lambda^\alpha, \quad \alpha \in (0, 1], \quad (50)$$

which corresponds to the Riemann-Liouville operator  $\mathcal{D} = {}_0D_t^{1-\alpha}$  in (3). In the top panel in Figure 1, we plot the protein concentration as a function of time for  $x = 1$  and  $\alpha = 2/3$ ,  $\alpha = 9/10$ , and  $\alpha = 1$  (the case  $\alpha = 1$  corresponds to normal diffusion). In the bottom panel in Figure 1, we plot the protein concentration as a function of space at a sequence of 3 time values. In these plots, we set  $k$ ,  $D$ , and  $\varphi$  to unity, and so the time, space, and concentrations can be interpreted as dimensionless.

From Figure 1, we see that (i) the protein concentration grows more quickly at early times for smaller values of  $\alpha$  and (ii) the protein concentration grows more slowly at later times for larger values of  $\alpha$ . In addition, the approach of the subdiffusive concentration  $c(x, t)$  to the steady-state  $u_{\text{ss}}(x)$  can be seen in Figure 1. However, we claim that the accumulation time formalism described above fails to quantify the timescale of this subdiffusive approach. To see this, define the subdiffusive accumulation time  $\tau_{\text{sub}}(x)$  analogously to the diffusive accumulation time in (46),

$$\tau_{\text{sub}}(x) := \int_0^\infty R_{\text{sub}}(x, t) dt,$$

where the subdiffusive local relaxation function  $R_{\text{sub}}(x, t)$  is defined analogously to (47),

$$R_{\text{sub}}(x, t) = \frac{c(x, t) - c_{\text{ss}}(x)}{c(x, 0) - c_{\text{ss}}(x)} = 1 - \frac{c(x, t)}{u_{\text{ss}}(x)}.$$

Using that  $\tau_{\text{sub}}(x)$  can be written in terms of the Laplace transform of  $R_{\text{sub}}(x, t)$  and using (49), we then obtain

$$\tau_{\text{sub}}(x) = \lim_{\lambda \rightarrow 0^+} \widehat{R_{\text{sub}}}(x, \lambda) = \tau(x) \lim_{\lambda \rightarrow 0^+} \frac{\Psi(\lambda)}{\lambda}.$$

Using the value  $\Psi(\lambda) = \lambda^\alpha$  in (50) corresponding to the Riemann-Liouville fractional derivative, we obtain that the accumulation time is infinite if  $\alpha \in (0, 1)$ ,

$$\tau_{\text{sub}}(x) = \infty. \quad (51)$$

The result in (51) is not surprising since  $\tau_{\text{sub}}(x)$  is defined analogously to a mean first passage time and it is known that subdiffusive processes typically have infinite mean first passage times [43].

Summarizing, compared to normal diffusion, we see that this subdiffusive model of gradient formation yields a protein concentration that grows faster at early times and slower at later times. Further, while the subdiffusive concentration approaches the diffusive steady state at large time, the accumulation time formalism does not describe this timescale.

## 4.2 Switching subdiffusivity

A variety of systems in cell biology are characterized by macromolecules whose diffusivity randomly switches between two or more discrete values [44]. For example, AMPA receptors on the post-synaptic membrane switch between fast diffusive and stationary modes [45]. Similarly, LFA-1 receptors switch between fast and slow diffusive modes [46, 47]. Indeed, the prevalence of such processes in cell biology is evidenced by the various statistical methods that have been created to study single particle tracking data and detect fluctuations in diffusion coefficients [46, 48, 49, 50, 51, 52, 47].

Switching diffusion coefficients often model (a) binding/unbinding of the diffusing particle to other molecules that alter its mobility or (b) switching conformations, with distinct mobilities corresponding to the effective sizes of the conformations [53, 54, 55]. If the motion of the particles is subdiffusive, and the factors causing the subdiffusion similarly hamper the transitions between states, then the spatiotemporal evolution of the particle population could be modeled by an equation of the form in (5). To illustrate, consider

$$\frac{\partial}{\partial t} \begin{pmatrix} c_0 \\ c_1 \end{pmatrix} = \mathcal{D} \Delta \begin{pmatrix} K_0 c_0 \\ K_1 c_1 \end{pmatrix} + \mathcal{D} \begin{pmatrix} -\lambda_0 & \lambda_1 \\ \lambda_0 & -\lambda_1 \end{pmatrix} \begin{pmatrix} c_0 \\ c_1 \end{pmatrix}, \quad (52)$$

which models a population of particles that switch between two states and subdiffuse in state  $j \in \{0, 1\}$  with generalized diffusivity  $K_j$ . If  $\mathcal{D} = {}_0D_t^{1-\alpha}$ , then section 3 shows that the dwell times in each state have the Mittag-Leffler distribution (see (40)).

Further, section 3 shows that the stochastic state of an individual particle following (52) is given by

$$(Y(t), J(t)) := (X(S(t)), I(S(t))) \in \bar{V} \times \{0, 1\},$$

where  $S(t)$  is the inverse of a subordinator  $T(s)$  with Lévy exponent given by the reciprocal of the Laplace transform of the memory kernel in  $\mathcal{D}$  (see section 2.1),  $I(s) \in \{0, 1\}$  is a two-state Markov jump process with jump rates  $\lambda_0, \lambda_1$ , and  $X(s)$  follows the switching SDE,

$$dX(s) = \sqrt{2K_{I(s)}} dW(s).$$

In Figure 2, we plot a realization of  $(Y(t), J(t))$  and the corresponding realizations of  $S(t)$ ,  $X(s)$ ,  $I(s)$ , and  $T(s)$  by employing the method described in section 3.3 above. In this plot, we take the fractional operator to be the Riemann-Liouville derivative,  $\mathcal{D} = {}_0D_t^{1-\alpha}$ , with  $\alpha = 3/4$ , and set  $\lambda_0 = \lambda_1$  and  $K_1/K_0 = 100$  so that the process moves much more quickly in state 1 compared to state 0.

In the top panel of Figure 2, we plot  $T$ ,  $I$ , and  $X$  as functions of the internal time  $s$ . Notice that  $T(s)$  is an increasing process which occasionally takes large jumps. Notice also that  $X(s)$  diffuses much faster when  $I(s) = 1$  compared to when  $I(s) = 0$ . In the bottom panel, we plot  $S$ ,  $J$ , and  $Y$  as functions of

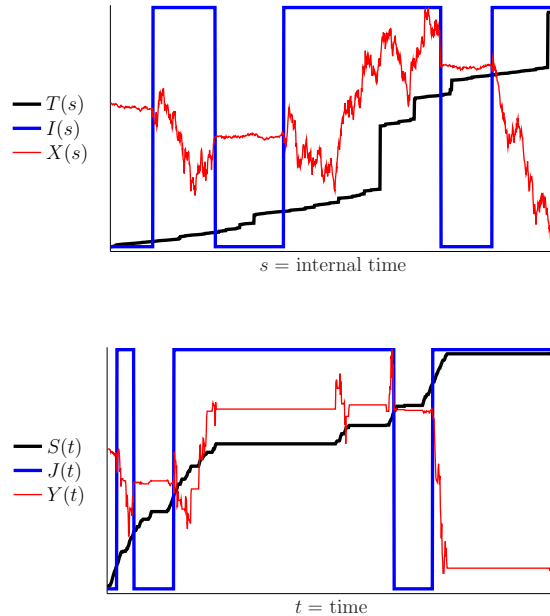


Figure 2: Switching subdiffusivity. In the top panel, we plot  $T(s)$ ,  $I(s)$ , and  $X(s)$  as functions of the internal time  $s$ . In the bottom panel, we plot  $S(t)$ ,  $J(t)$ , and  $Y(t)$  as functions of time  $t$ . See the text for details.

time  $t$ . Notice that jumps in  $T$  correspond to flat periods or “pauses” in  $S$ . Notice also that both  $J$  and  $Y$  pause when  $S$  pauses. In particular, though  $I(s)$  switches states at exponentially distributed times, the pauses in  $J(t)$  induced by  $S(t)$  make  $J(t)$  switch states at Mittag-Leffler distributed times (see (40)). Furthermore, notice that if  $Y$  is not paused, then it moves much more quickly when  $J(t) = 1$  compared to when  $J(t) = 0$ . We note that we have shifted and scaled the vertical axes in Figure 2 so that the various curves fit on the same plots.

### 4.3 Space-dependent switching and gradient formation

In the example in section 4.2 above, the particles switch states at rates that are independent of their spatial position. It was recently shown that space-dependent switching can induce the formation of protein concentration gradients inside a single cell [54]. This mechanism of gradient formation is particularly notable since the more classical mechanism involving diffusion away from a localized source and subsequent degradation (as in section 4.1 above) typically fails at subcellular length scales [56, 57].

This situation has been modeled by [54, 58]

$$\frac{\partial}{\partial s} \begin{pmatrix} u_0 \\ u_1 \end{pmatrix} = \Delta \begin{pmatrix} K_0 u_0 \\ K_1 u_1 \end{pmatrix} + \frac{1}{\varepsilon} \begin{pmatrix} -\lambda_0(x) & \lambda_1(x) \\ \lambda_0(x) & -\lambda_1(x) \end{pmatrix} \begin{pmatrix} u_0 \\ u_1 \end{pmatrix}, \quad (53)$$

where  $u_j(x, s)$  is the concentration of molecules in state  $j \in \{0, 1\}$  at time  $s \geq 0$  at position  $x$  in the finite interval  $[0, L]$ . Notice that the rate  $\lambda_j(x)$  of leaving state  $j$  depends on the current spatial position. In (53), a small dimensionless parameter  $\varepsilon > 0$  has been introduced to model switching that occurs on a much faster timescale than gradient formation. It was shown in [58] that if  $\varepsilon \ll 1$ , then the large time total concentration  $u(x) := \lim_{s \rightarrow \infty} u_0(x, s) + u_1(x, s)$  is proportional to

$$u(x) \propto \left( \frac{\lambda_1(x)}{\lambda_0(x) + \lambda_1(x)} K_0 + \frac{\lambda_0(x)}{\lambda_0(x) + \lambda_1(x)} K_1 \right)^{-1}, \quad (54)$$

assuming no flux boundary conditions for  $u_j$  at  $x = 0, L$ . The form in (54) means that molecules concentrate in regions where they are more likely to be in a slower state. This point is related to a fairly subtle point regarding Itô versus Stratonovich stochastic integration [59, 60].

Given the ubiquity of subdiffusive motion inside cells, it is natural to ask if this same mechanism for gradient formation exists for subdiffusion. If the reactions causing the transitions between states is subdiffusion-limited, then the concentrations  $c_0(x, t)$  and  $c_1(x, t)$  can be modeled by the equations in (53) with the operator  $\mathcal{D}$  applied to the righthand side. Our analysis in section 2 thus shows that the subdiffusive concentrations are  $c_j(x, t) = \mathbb{E}[u_j(x, S(t))]$ . It then follows from our analysis in section 2.4 that the large time total subdiffusive concentration is exactly given by (54), which shows that this mechanism of intracellular gradient formation extends to subdiffusive motion.

#### 4.4 FRAP experiments

Fluorescence recovery after photobleaching (FRAP) is a commonly used experimental method for studying binding interactions in cells [61]. Though subdiffusion is widely observed in cells, the vast majority of mathematical models of FRAP experiments assume that the molecules move by normal diffusion (but see the work of Yuste et al. [62] for a notable exception).

In the case of normal diffusion, the influential work of Sprague et al. [63] considers the following linear reaction-diffusion equations describing a FRAP system in a two-dimensional disk,

$$\begin{aligned} \frac{\partial u_0}{\partial s} &= D \left( \frac{1}{r} \frac{\partial}{\partial r} + \frac{\partial^2}{\partial r^2} \right) u_0 - k_{\text{on}} u_0 + k_{\text{off}} u_1, \\ \frac{\partial u_1}{\partial s} &= k_{\text{on}} u_0 - k_{\text{off}} u_1, \end{aligned} \quad (55)$$

for free (respectively bound) proteins  $u_0(r, s)$  (respectively  $u_1(r, s)$ ) at radius  $r \in (0, \rho)$  at time  $s \geq 0$ . In order to compare to experimental data, one calculates

the so-called FRAP curve, which is the sum  $u_0 + u_1$  averaged over the disk,

$$\text{frap}(s) := \frac{2}{\rho^2} \int_0^\rho \left( u_0(r, s) + u_1(r, s) \right) r \, dr. \quad (56)$$

While an explicit formula for (56) is unknown, Sprague et al. [63] found the following exact formula for its Laplace transform,

$$\begin{aligned} \widehat{\text{frap}}(\lambda) &= \frac{1}{\lambda} - \frac{k_{\text{on}}}{(\lambda + k_{\text{off}})(k_{\text{on}} + k_{\text{off}})} \\ &\quad - \frac{k_{\text{off}}}{\lambda(k_{\text{on}} + k_{\text{off}})} \left( 1 - 2K_1(q\rho)I_1(q\rho) \right) \left( 1 + \frac{k_{\text{on}}}{\lambda + k_{\text{off}}} \right), \end{aligned} \quad (57)$$

where  $I_1$  and  $K_1$  are modified Bessel functions of the first and second kind and

$$q = \sqrt{\frac{\lambda}{D} \left( 1 + \frac{k_{\text{on}}}{\lambda + k_{\text{off}}} \right)}.$$

Note that (57) has been normalized so that it yields  $\lim_{s \rightarrow \infty} \text{frap}(s) = 1$ . The Laplace transform (57) can be inverted numerically to yield the FRAP curve (56) and then be compared to experimental data [63].

We can extend these results to the case that the proteins move by subdiffusion and the reactions are subdiffusion-limited. In particular, suppose the subdiffusion is modeled with the fractional operator  $\mathcal{D}$  in (6). Let  $\text{frap}_{\text{sub}}(t)$  denote the subdiffusive FRAP curve defined as in (56), but where  $u_0$  and  $u_1$  are replaced by  $c_0$  and  $c_1$  which satisfy (55) with  $\mathcal{D}$  applied to the righthand sides. Theorem 1 then implies that the Laplace transform of the subdiffusive FRAP curve is given explicitly in terms of (57),

$$\widehat{\text{frap}}_{\text{sub}}(\lambda) = \frac{\Psi(\lambda)}{\lambda} \widehat{\text{frap}}(\Psi(\lambda)), \quad \lambda > 0, \quad (58)$$

where  $\Psi(\lambda)$  corresponds to  $\mathcal{D}$  (see section 2.1). As above, (58) can be inverted numerically to yield the subdiffusive FRAP curve.

In Figure 3, we plot the diffusive FRAP curve and the subdiffusive FRAP curve as functions of time. The circles in the top panel in Figure 3 are experimental data points from Figure 5E in [63]. Similarly, the circles in the bottom panel in Figure 3 are data points from Figure 5F in [63]. Figure 3 shows that the subdiffusion-limited FRAP model described above can fit this experimental data of [63]. This figure follows Figures 1 and 2 in [62] that showed that a different subdiffusive FRAP model can also fit this experimental data of [63].

The parameters used in Figure 3 are as follows. In Figure 3, the radius is  $\rho = 1.1 \mu\text{m}$  in the top panel and  $\rho = 0.5 \mu\text{m}$  in the bottom panel. For diffusive FRAP (blue solid curves), we take  $k_{\text{on}} = 400 \text{ sec}^{-1}$ ,  $k_{\text{off}} = 78.6 \text{ sec}^{-1}$ , and  $D = 9.2 \mu\text{m}^2 \text{ sec}^{-1}$  in both panels. For the subdiffusive FRAP (red dashed curves), we take the fractional operator to be the Riemann-Liouville operator  $\mathcal{D} = {}_0D_t^{1-\alpha}$  with  $\alpha = 0.75$ , and set  $k_{\text{on}} = 750 \text{ sec}^{-\alpha}$ ,  $k_{\text{off}} = 17 \text{ sec}^{-\alpha}$ , and  $D = 82 \mu\text{m}^2 \text{ sec}^{-\alpha}$  in both panels. The parameters for the diffusive FRAP curves were used in Figure 5F in [63] (slightly different parameters were used in Figure 5E in [63], but we use the same parameters in both panels).

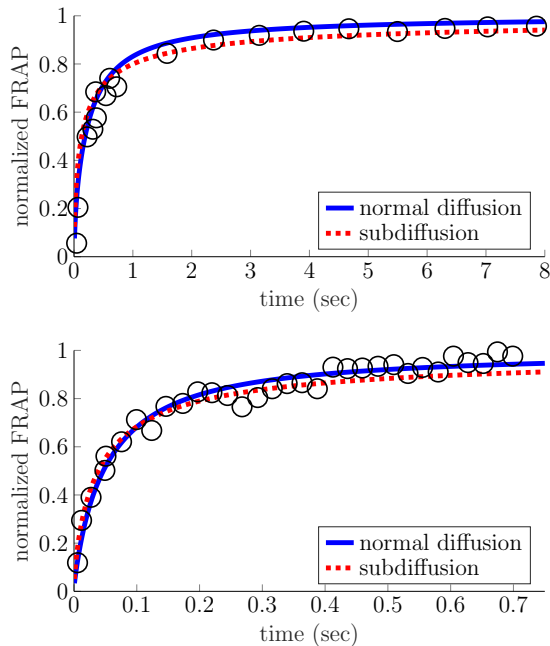


Figure 3: FRAP curves for normal diffusion (blue solid) and subdiffusion (red dashed) can fit experimental data (black circles) of [63]. See the text for details.

## 5 Fractional ODEs

Our results hold in significant generality, essentially requiring only that the operator  $\mathcal{A}$  commutes with temporal operators (see (23)-(25)). Indeed, the equations need not even involve the spatial variable  $x$ , and can instead be a system of fractional ODEs. Fractional ODEs have been used to model a variety of systems, including pharmacokinetics [64] and the spread of an infectious disease through a population [65].

### 5.1 Solution

Consider the affine fractional ODEs,

$$\frac{d}{dt}\mathbf{c}(t) = \mathcal{D}(R\mathbf{c}(t) + \mathbf{r}), \quad (59)$$

where  $\mathbf{c}(t) = (c_i(t))_{i=1}^n \in \mathbb{R}^n$  is a time-dependent solution vector and  $R \in \mathbb{R}^{n \times n}$  is a matrix and  $\mathbf{r} \in \mathbb{R}^n$  is a vector. In this case, section 2 yields the relations

$$\begin{aligned} \mathbf{c}(t) &= \mathbb{E}[\mathbf{u}(S(t))], \\ \hat{\mathbf{c}}(\lambda) &= \frac{\Psi(\lambda)}{\lambda} \hat{\mathbf{u}}(\Psi(\lambda)), \end{aligned} \quad (60)$$

as in (10)-(11), where  $\mathbf{u}$  satisfies the ODE

$$\frac{d}{ds}\mathbf{u}(s) = R\mathbf{u}(s) + \mathbf{r}, \quad (61)$$

with  $\mathbf{u}(0) = \mathbf{c}(0) \in \mathbb{R}^n$ .

The solution  $\mathbf{u}(s)$  to (61) is of course

$$\mathbf{u}(s) = e^{Rs}\mathbf{u}(0) + \int_0^s e^{R(s-\sigma)}\mathbf{r} d\sigma = \sum_{k=0}^{\infty} \frac{R^k s^k}{k!} \mathbf{u}(0) + \sum_{k=0}^{\infty} \frac{R^k s^{k+1}}{(k+1)!} \mathbf{r}.$$

Hence, (60) yields the following explicit formula for the fractional solution in terms of the moments of  $S(t)$ ,

$$\mathbf{c}(t) = \sum_{k=0}^{\infty} \frac{R^k \mathbb{E}[(S(t))^k]}{k!} \mathbf{c}(0) + \sum_{k=0}^{\infty} \frac{R^k \mathbb{E}[(S(t))^{k+1}]}{(k+1)!} \mathbf{r}. \quad (62)$$

In the case that the fractional operator is the Riemann-Liouville derivative,  $\mathcal{D} = {}_0D_t^{1-\alpha}$ , we have that [66]

$$\mathbb{E}[(S(t))^k] = \frac{t^{\alpha k} k!}{\Gamma(1 + \alpha k)}. \quad (63)$$

Plugging (63) into (62) yields a formula for  $\mathbf{c}(t)$  that agrees with a recent result of Duan [67].

## 5.2 Stability

Equations (32)-(33) in section 2.4 above show that if  $\mathbf{u}$  approaches a finite limit at large time, then  $\mathbf{c}$  must also approach this same limit at large time. Furthermore, the results of section 2.4 yield that if a nonlinear integer order ODE is linearly stable, then the corresponding nonlinear fractional order ODE is also linearly stable.

However, we caution that the stability of an integer order ODE cannot be inferred from the stability of the corresponding fractional ODE. Indeed, if the fractional operator is the Riemann-Liouville operator,  $\mathcal{D} = {}_0D_t^{1-\alpha}$ , then it is known [68, 69] that the origin is asymptotically stable for the linear fractional ODE

$$\frac{d}{dt}\mathbf{c}(t) = {}_0D_t^{1-\alpha} R\mathbf{c}(t), \quad (64)$$

if and only if

$$|\text{Arg}(\nu)| > \frac{\alpha\pi}{2}, \quad (65)$$

for every eigenvalue  $\nu \in \mathbb{C}$  of  $R \in \mathbb{R}^{n \times n}$ , where  $\text{Arg}(\nu) \in (-\pi, \pi]$  denotes the principal argument of  $\nu$ . Notice that (65) generalizes the classical result for integer order ODEs with  $\alpha = 1$ . Hence, if  $R$  satisfies (65) and

$$|\text{Arg}(\nu)| < \frac{\pi}{2},$$

for some  $\nu \in \mathbb{C}$ , then the solution to (64) vanishes but the solution to the corresponding integer equation diverges.

### 5.3 Stochastic representation

The stochastic representation of section 3 above still holds in the non-spatial case of (59) if  $\mathbf{r} = 0$  and  $R$  is the forward operator for a continuous-time Markov chain (as in section 3). In this case, if  $\{I(s)\}_{s \geq 0}$  is a continuous-time Markov chain with forward operator  $R$ , then the probability distribution of  $J(t) := I(S(t))$  satisfies (59) with  $\mathbf{r} = 0$ . We note that this connection between fractional order and integer order Markov chains was investigated in [70, 71, 72, 73, 74, 75, 76, 77, 34] in the case that  $\mathcal{D}$  is the Riemann-Liouville derivative and  $\{I(s)\}_{s \geq 0}$  is a Poisson process.

## 6 Discussion

We have analyzed subdiffusion-limited mesoscopic equations describing a reaction-subdiffusion system in a general mathematical setting, under the assumption that the reactions are affine. We have shown that the solution to this fractional system is the expectation of a random time change of the corresponding integer order system. This result yielded (i) a simple algebraic relation between the fractional solution and the integer order solution in Laplace space, (ii) a sufficient condition for the stability of fractional equations with nonlinear reactions in terms of the stability of the corresponding integer order equations, and (iii) the exact microscopic description of single molecules corresponding to these mesoscopic equations and a numerical method for their stochastic simulation.

These results extend previous results for subdiffusive systems with no reactions. Barkai [78] found the solution to a fractional Fokker-Planck equation in  $\mathbb{R}$  in terms of the solution to the corresponding integer order Fokker-Planck equation in the case that the fractional operator is the Riemann-Liouville derivative. Magdziarz [79] found the stochastic representation for such fractional Fokker-Planck equations in  $\mathbb{R}$  when the fractional operator involves a general memory kernel. This was further generalized in [80] by Magdziarz and Zorawik. In addition, fractional Fokker-Planck equations in  $\mathbb{R}^d$  with general memory kernels were considered by Carnaffan and Kawai [38]. Similar stochastic representations of solutions to fractional equations have been found in [81, 82, 83, 84].

We used our results to explore how subdiffusion modifies several models in cell biology. The Laplace space relation we found between solutions to fractional and integer order equations allowed us to quickly convert results from diffusive models to subdiffusive models. Our results suggest that mechanisms for gradient formation which have been formulated for diffusive molecules extend to subdiffusive molecules. In addition, it is interesting that our subdiffusive FRAP model closely fits data from FRAP experiments [63]. This parallels the work of Yuste et al. [62], which found similar results for a different subdiffusive FRAP model.

We also applied our results to fractional ODEs. Our work extends recent solution formulas for fractional ODEs [67] to more general fractional operators. In addition, our work complements and extends some previous work on fractional Poisson processes [70, 71, 72, 73, 74, 75, 76, 77, 34].

While our results are formulated in significant mathematical generality, we did assume that the reactions are affine functions (except in our stability results). In contrast, some previous studies considered models with nonlinear reactions (often mass action kinetics) [21, 23, 24, 14, 26, 25, 27]. Hence, further investigating the relationship between fractional and integer order equations involving nonlinearities remains an important direction for future work.

## Acknowledgments

The author gratefully acknowledges support from the National Science Foundation (DMS-1944574, DMS-1814832, and DMS-1148230).

## References

- [1] Fernando A Oliveira, Rogelma Ferreira, Luciano C Lapas, and Mendeli H Vainstein. Anomalous diffusion: A basic mechanism for the evolution of inhomogeneous systems. *Frontiers in Physics*, 7:18, 2019.
- [2] Joseph Klafter and Igor M Sokolov. Anomalous diffusion spreads its wings. *Physics world*, 18(8):29, 2005.
- [3] Igor M Sokolov. Models of anomalous diffusion in crowded environments. *Soft Matter*, 8(35):9043–9052, 2012.
- [4] Yasmine Meroz and Igor M Sokolov. A toolbox for determining subdiffusive mechanisms. *Physics Reports*, 573:1–29, 2015.
- [5] Felix Höfling and Thomas Franosch. Anomalous transport in the crowded world of biological cells. *Reports on Progress in Physics*, 76(4):046602, 2013.
- [6] Eli Barkai, Yuval Garini, and Ralf Metzler. Strange kinetics of single molecules in living cells. *Phys. Today*, 65(8):29, 2012.
- [7] Ralf Metzler and Joseph Klafter. The random walk’s guide to anomalous diffusion: a fractional dynamics approach. *Physics reports*, 339(1):1–77, 2000.
- [8] Stefan G Samko, Anatoly A Kilbas, Oleg I Marichev, et al. *Fractional integrals and derivatives*, volume 1. Gordon and Breach Science Publishers, Yverdon Yverdon-les-Bains, Switzerland, 1993.
- [9] AA Nepomnyashchy. Mathematical modelling of subdiffusion-reaction systems. *Mathematical Modelling of Natural Phenomena*, 11(1):26–36, 2016.

- [10] Gil Hornung, Brian Berkowitz, and Naama Barkai. Morphogen gradient formation in a complex environment: an anomalous diffusion model. *Physical Review E*, 72(4):041916, 2005.
- [11] VV Gafiychuk and BY Datsko. Spatiotemporal pattern formation in fractional reaction-diffusion systems with indices of different order. *Physical Review E*, 77(6):066210, 2008.
- [12] Jean Pierre Boon, James F Lutsko, and Christopher Lutsko. Microscopic approach to nonlinear reaction-diffusion: The case of morphogen gradient formation. *Physical Review E*, 85(2):021126, 2012.
- [13] Christopher N Angstmann, Isaac C Donnelly, and Bruce I Henry. Continuous time random walks with reactions forcing and trapping. *Mathematical Modelling of Natural Phenomena*, 8(2):17–27, 2013.
- [14] T Kosztolowicz and KD Lewandowska. Application of fractional differential equations in modelling the subdiffusion–reaction process. *Mathematical Modelling of Natural Phenomena*, 8(2):44–54, 2013.
- [15] Scott K Hansen and Brian Berkowitz. Integrodifferential formulations of the continuous-time random walk for solute transport subject to bimolecular  $a + b \rightarrow 0$  reactions: From micro-to mesoscopic. *Physical Review E*, 91(3):032113, 2015.
- [16] Peter Straka and Sergei Fedotov. Transport equations for subdiffusion with nonlinear particle interaction. *Journal of theoretical biology*, 366:71–83, 2015.
- [17] Maike AF Dos Santos. From continuous-time random walks to controlled-diffusion reaction. *Journal of Statistical Mechanics: Theory and Experiment*, 2019(3):033214, 2019.
- [18] Wen-Biao Zhang and Ming Yi. Reaction-anomalous diffusion processes for  $a + b \rightleftharpoons c$ . *Physica A: Statistical Mechanics and its Applications*, 527:121347, 2019.
- [19] GH Li, H Zhang, and B Zhang. Continuous time random walk with  $a \rightarrow b$  reaction in flows. *Physica A: Statistical Mechanics and its Applications*, 532:121917, 2019.
- [20] Kazuhiko Seki, Mariusz Wojcik, and M Tachiya. Recombination kinetics in subdiffusive media. *The Journal of chemical physics*, 119(14):7525–7533, 2003.
- [21] SB Yuste, L Acedo, and Katja Lindenberg. Reaction front in an  $a + b \rightarrow c$  reaction-subdiffusion process. *Physical Review E*, 69(3):036126, 2004.
- [22] BI Henry, TAM Langlands, and SL Wearne. Anomalous diffusion with linear reaction dynamics: From continuous time random walks to fractional reaction-diffusion equations. *Physical Review E*, 74(3):031116, 2006.

- [23] Tadeusz Kosztołowicz and Katarzyna D Lewandowska. Time evolution of the reaction front in the system with one static and one subdiffusive reactant. *Acta Phys. Pol. B*, 37(5):1571–1578, 2006.
- [24] Tadeusz Kosztołowicz and Katarzyna D Lewandowska. Time evolution of the reaction front in a subdiffusive system. *Physical Review E*, 78(6):066103, 2008.
- [25] Yana Nec and Michael J Ward. An explicitly solvable nonlocal eigenvalue problem and the stability of a spike for a sub-diffusive reaction-diffusion system. *Mathematical Modelling of Natural Phenomena*, 8(2):55–87, 2013.
- [26] Yana Nec, Vladimir A Volpert, and Alexander A Nepomnyashchy. Front propagation problems with sub-diffusion. *Discr. Cont. Dyn. Sys. Series A*, 27(2):827–846, 2010.
- [27] AA Nepomnyashchy and VA Volpert. An exactly solvable model of subdiffusion–reaction front propagation. *Journal of Physics A: Mathematical and Theoretical*, 46(6):065101, 2013.
- [28] Ralf Metzler, Eli Barkai, and Joseph Klafter. Anomalous diffusion and relaxation close to thermal equilibrium: A fractional Fokker-Planck equation approach. *Physical review letters*, 82(18):3563, 1999.
- [29] Jean Bertoin. *Lévy processes*, volume 121. Cambridge university press Cambridge, 1996.
- [30] Ken-Iti Sato. *Lévy processes and infinitely divisible distributions*. Cambridge university press, 1999.
- [31] Lorenzo Farina and Sergio Rinaldi. *Positive linear systems: theory and applications*, volume 50. John Wiley & Sons, 2011.
- [32] G. Yin and C. Zhu. *Hybrid Switching Diffusions*. Springer, New York, USA, 2010.
- [33] RN Pillai. On mittag-leffler functions and related distributions. *Annals of the Institute of statistical Mathematics*, 42(1):157–161, 1990.
- [34] Mark Meerschaert, Erkan Nane, P Vellaisamy, et al. The fractional poisson process and the inverse stable subordinator. *Electronic Journal of Probability*, 16:1600–1620, 2011.
- [35] Daniel T Gillespie. Exact stochastic simulation of coupled chemical reactions. *The journal of physical chemistry*, 81(25):2340–2361, 1977.
- [36] Peter E Kloeden and Eckhard Platen. *Numerical solution of stochastic differential equations*, volume 23. Springer Science & Business Media, 2013.

- [37] Marcin Magdziarz, Aleksander Weron, and Karina Weron. Fractional fokker-planck dynamics: Stochastic representation and computer simulation. *Physical Review E*, 75(1):016708, 2007.
- [38] Sean Carnaffan and Reiiichiro Kawai. Solving multidimensional fractional Fokker–Planck equations via unbiased density formulas for anomalous diffusion processes. *SIAM Journal on Scientific Computing*, 39(5):B886–B915, 2017.
- [39] Aude Porcher and Nathalie Dostatni. The bicoid morphogen system. *Current biology*, 20(5):R249–R254, 2010.
- [40] Alexander M Berezhkovskii, Christine Sample, and Stanislav Y Shvartsman. How long does it take to establish a morphogen gradient? *Biophysical journal*, 99(8):L59–L61, 2010.
- [41] Sven Bergmann, Oded Sandler, Hila Sberro, Sara Shnider, Eyal Schejter, Ben-Zion Shilo, and Naama Barkai. Pre-steady-state decoding of the bicoid morphogen gradient. *PLoS Biol*, 5(2):e46, 2007.
- [42] Alexander M Berezhkovskii, Christine Sample, and Stanislav Y Shvartsman. Formation of morphogen gradients: Local accumulation time. *Physical Review E*, 83(5):051906, 2011.
- [43] SB Yuste and Katja Lindenberg. Comment on “Mean first passage time for anomalous diffusion”. *Physical Review E*, 69(3):033101, 2004.
- [44] P. C. Bressloff. *Stochastic Processes in Cell Biology*. Springer International Publishing, 2014.
- [45] A J Borgdorff and D Choquet. Regulation of AMPA receptor lateral movements. *Nature*, 417(6889):649, 2002.
- [46] R Das, C W Cairo, and D Coombs. A hidden markov model for single particle tracks quantifies dynamic interactions between LFA-1 and the actin cytoskeleton. *PLoS Comput Biol*, 5(11):e1000556, 2009.
- [47] P J Slator, C W Cairo, and N J Burroughs. Detection of diffusion heterogeneity in single particle tracking trajectories using a hidden markov model with measurement noise propagation. *PLoS One*, 10(10):e0140759, 2015.
- [48] P K Koo and S G J Mochrie. Systems-level approach to uncovering diffusive states and their transitions from single-particle trajectories. *Phys Rev E*, 94(5):052412, 2016.
- [49] Nilah Monnier. *Bayesian Inference Approaches for Particle Trajectory Analysis in Cell Biology*. PhD thesis, Harvard University, 2013.
- [50] D Montiel, H Cang, and H Yang. Quantitative characterization of changes in dynamical behavior for single-particle tracking studies. *J Phys Chem B*, 110(40):19763–19770, 2006.

- [51] F Persson, M Lindén, C Unoson, and J Elf. Extracting intracellular diffusive states and transition rates from single-molecule tracking data. *Nat Methods*, 10(3):265, 2013.
- [52] P J Slator and N Burroughs. A hidden markov model for detecting confinement in single particle tracking trajectories. *bioRxiv*, page 275107, 2018.
- [53] C W Cairo, R Mirchev, and D E Golan. Cytoskeletal regulation couples lfa-1 conformational changes to receptor lateral mobility and clustering. *Immunity*, 25(2):297–308, 2006.
- [54] Y Wu, B Han, Y Li, E Munro, D J Odde, and E E Griffin. Rapid diffusion-state switching underlies stable cytoplasmic gradients in the caenorhabditis elegans zygote. *Proc Natl Acad Sci*, page 201722162, 2018.
- [55] Denis S Grebenkov. Time-averaged mean square displacement for switching diffusion. *Physical Review E*, 99(3):032133, 2019.
- [56] Boris N Kholodenko. Spatially distributed cell signalling. *FEBS letters*, 583(24):4006–4012, 2009.
- [57] M Howard. How to build a robust intracellular concentration gradient. *Trends Cell Biol*, 22(6):311–317, 2012.
- [58] P C Bressloff, S D Lawley, and P Murphy. Protein concentration gradients and switching diffusions. *Phys Rev E*, 99(3):032409, 2019.
- [59] P C Bressloff and S D Lawley. Temporal disorder as a mechanism for spatially heterogeneous diffusion. *Phys Rev E - Rapid Comm*, 95(6):060101, 2017.
- [60] P C Bressloff and S D Lawley. Hybrid colored noise process with space-dependent switching rates. *Phys Rev E*, 96(1):012129, 2017.
- [61] Jennifer Lippincott-Schwartz, Erik Lee Snapp, and Robert D Phair. The development and enhancement of frap as a key tool for investigating protein dynamics. *Biophysical journal*, 115(7):1146–1155, 2018.
- [62] SB Yuste, E Abad, and K Lindenberg. A reaction–subdiffusion model of fluorescence recovery after photobleaching (frap). *Journal of Statistical Mechanics: Theory and Experiment*, 2014(11):P11014, 2014.
- [63] Brian L Sprague, Robert L Pego, Diana A Stavreva, and James G McNally. Analysis of binding reactions by fluorescence recovery after photobleaching. *Biophysical journal*, 86(6):3473–3495, 2004.
- [64] Aristides Dokoumetzidis and Panos Macheras. Fractional kinetics in drug absorption and disposition processes. *Journal of pharmacokinetics and pharmacodynamics*, 36(2):165–178, 2009.

- [65] Christopher N Angstmann, Austen M Erickson, Bruce I Henry, Anna V McGann, John M Murray, and James A Nichols. Fractional order compartment models. *SIAM Journal on Applied Mathematics*, 77(2):430–446, 2017.
- [66] A Piryatinska, AI Saichev, and WA Woyczynski. Models of anomalous diffusion: the subdiffusive case. *Physica A: Statistical Mechanics and its Applications*, 349(3-4):375–420, 2005.
- [67] Junsheng Duan. System of linear fractional differential equations and the mittag-leffler functions with matrix variable. In *J. Phys. Conf. Ser.*, volume 1053, 2018.
- [68] Denis Matignon. Stability results for fractional differential equations with applications to control processing. In *Computational engineering in systems applications*, volume 2, pages 963–968. Lille, France, 1996.
- [69] CP Li and FR Zhang. A survey on the stability of fractional differential equations. *The European Physical Journal Special Topics*, 193(1):27–47, 2011.
- [70] ON Repin and AI Saichev. Fractional poisson law. *Radiophysics and Quantum Electronics*, 43(9):738–741, 2000.
- [71] Guy Jumarie. Fractional master equation: non-standard analysis and liouville–riemann derivative. *Chaos, Solitons & Fractals*, 12(13):2577–2587, 2001.
- [72] Nick Laskin. Fractional poisson process. *Communications in Nonlinear Science and Numerical Simulation*, 8(3-4):201–213, 2003.
- [73] Francesco Mainardi, Rudolf Gorenflo, and E Scalas. A fractional generalization of the poisson processes. *Vietnam J Math*, 32:53–64, 2004.
- [74] Francesco Mainardi, Rudolf Gorenflo, and Alessandro Vivoli. Beyond the poisson renewal process: A tutorial survey. *Journal of Computational and Applied Mathematics*, 205(2):725–735, 2007.
- [75] Vladimir V Uchaikin, Dexter O Cahoy, and Renat T Sibatov. Fractional processes: from poisson to branching one. *International Journal of Bifurcation and Chaos*, 18(09):2717–2725, 2008.
- [76] Luisa Beghin, Enzo Orsingher, et al. Fractional poisson processes and related planar random motions. *Electronic Journal of Probability*, 14:1790–1826, 2009.
- [77] Luisa Beghin, Enzo Orsingher, et al. Poisson-type processes governed by fractional and higher-order recursive differential equations. *Electronic Journal of Probability*, 15:684–709, 2010.

- [78] E Barkai. Fractional fokker-planck equation, solution, and application. *Physical Review E*, 63(4):046118, 2001.
- [79] Marcin Magdziarz. Langevin picture of subdiffusion with infinitely divisible waiting times. *Journal of Statistical Physics*, 135(4):763–772, 2009.
- [80] Marcin Magdziarz and Tomasz Zorawik. Stochastic representation of a fractional subdiffusion equation. the case of infinitely divisible waiting times, lévy noise and space-time-dependent coefficients. *Proceedings of the American Mathematical Society*, 144(4):1767–1778, 2016.
- [81] Boris Baeumer and Mark M Meerschaert. Stochastic solutions for fractional cauchy problems. *Fractional Calculus and Applied Analysis*, 4(4):481–500, 2001.
- [82] Mark M Meerschaert and Hans-Peter Scheffler. Limit theorems for continuous-time random walks with infinite mean waiting times. *Journal of applied probability*, pages 623–638, 2004.
- [83] Zhen-Qing Chen. Time fractional equations and probabilistic representation. *Chaos, Solitons & Fractals*, 102:168–174, 2017.
- [84] Qiang Du, Lorenzo Toniazzi, and Zhi Zhou. Stochastic representation of solution to nonlocal-in-time diffusion. *Stochastic Processes and their Applications*, 130(4):2058–2085, 2020.